

PREDICTABILITY OF TROPICAL CYCLONES: A COMPARISON OF TYPHOON HAIYAN (2013) AND TYPHOON HAGUPIT (2014) USING CONVECTION-PERMITTING ENSEMBLE FORECASTS

John Ashcroft¹ *, Juliane Schwendike¹, Andrew Ross¹, Stephen Griffiths¹, Chris Short²

¹ University of Leeds, Leeds, UK

²Met Office, Exeter, UK

1 INTRODUCTION

Whilst accurately forecasting the intensity of tropical cyclones (TCs) remains a major challenge, track forecasts have improved considerably over the past few decades. However, there remain cases where numerical weather prediction models have been unable to accurately forecast the motion of a storm. Typhoon Hagupit (2014) is one such TC where, a few days prior to making landfall over the Philippines, operational ensemble forecasts showed large uncertainty in its future track. In contrast the spread of tracks from ensemble forecasts for Typhoon Haiyan (2013) were considerably less. Both TCs reached the equivalent of a category-5 hurricane and both followed similar tracks across the Pacific before making landfall.

Using global and regional ensemble forecasts a comparison between the two storms is made to investigate the reasons for the poorer predictability of Hagupit.

2 MODEL SET UP

The Met Office's Unified Model was used to produce both 4.4-km, limited-area, convection-permitting (CP), 5 day ensemble forecasts and 5 day global ensemble forecasts. The global forecasts were generated by the Met Office Global and Regional Ensemble Prediction System (MOGREPS-G, 800×600 grid points, 70 vertical levels). The convection permitting ensemble (0.04° resolution, 80 vertical levels) is produced by nesting down each member of the global ensemble. The locations of the one-way nested grid for each storm is shown in Figure 1. No perturbations are made to the model physics, thus the only

perturbations in the CP ensembles are inherited from the global ensemble.

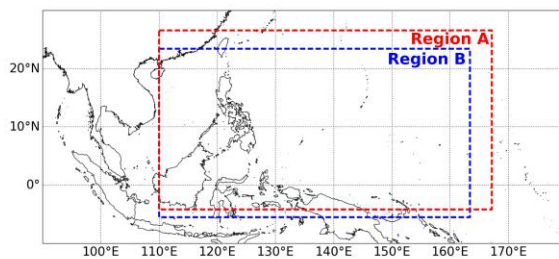


Figure 1: Location of the 4.4km nested grid for the CP simulations for Haiyan (Region A) and Hagupit (Region B).

Forecasts were initialised at 12 hr intervals from 0 Z, 4/11/2013 to 12 Z 8/1/2013 for Haiyan and 0 Z, 2/12/2014 to 12 Z 7/12/2014 for Hagupit. Here, results are shown from the forecasts initialised at 12 Z, 4/11/2013 and 12 Z, 3/12/2014 for Haiyan and Hagupit respectively.

3 TRACK AND INTENSITY

Global forecasts show there was much greater uncertainty in the track of Hagupit compared to Haiyan (Figures 2a and 2b). The 4.4-km forecasts (Figures 2c and 2d) show little spread in the forecasted tracks of both storms, however, all of the track forecasts for Hagupit deviate from the best track line due to a systematic turn towards the south before making landfall.

The intensity predictions for both storms were limited by a weak initialisation of the storm (Figure 3). In the global forecasts both storms remained very weak and showed little intensification. The 4.4-km forecasts produced a much better intensifi-

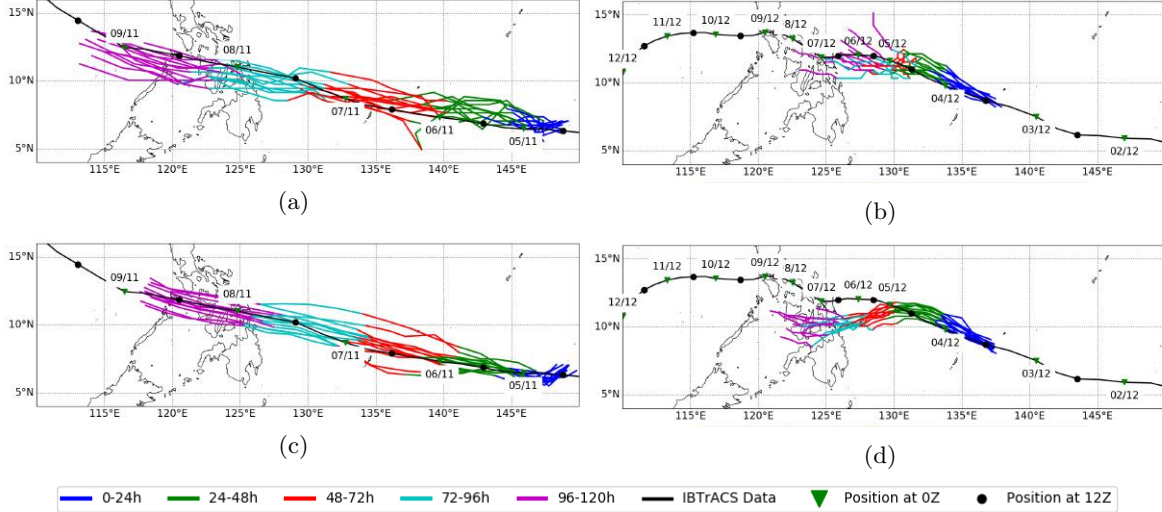


Figure 2: Track forecast results for (left) Haiyan and (right) Hagupit from both the (top) global forecasts and (bottom) CP 4.4-km forecasts. The black lines represent the best track according to IBTrACS. The location of the storm is determined using maximum relative vorticity at 850 hPa and minimum sea level pressure, using the algorithm outlined in Heming (2017).

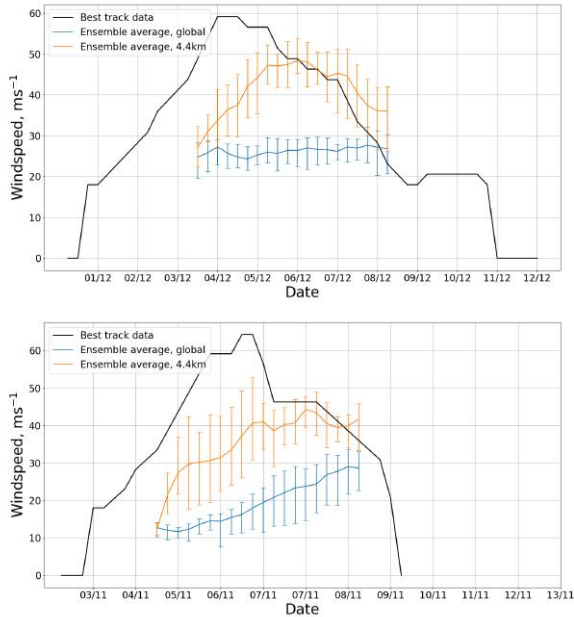


Figure 3: Intensity forecasts of (top) Haiyan and (bottom) Hagupit using the maximum 10-m wind speed. Error bars show the range of intensities in the ensemble.

cation of both storms, however they still failed to reach the peak intensities.

By comparing the track and intensity forecasts of both storms in the global and CP simulations, other important features can be outlined:

- The propagation speed of Haiyan is much greater than that of Hagupit.

- The spread of tracks is greater for the global forecasts compared to the 4.4-km forecasts. However the intensity spread is greater for the 4.4-km forecasts.
- The track forecasts for Hagupit show there is one region and time (approximately 12Z, 5/12/2014) at which the different ensemble members begin to deviate.

4 ENVIRONMENTAL CONDITIONS

Haiyan moved in a straight line across the Pacific and towards the Philippines along the southern periphery of the subtropical ridge (Figure 4). Hagupit was also initially steered by a high pressure ridge, with the storm located to the southwest of this ridge. However, as Hagupit moved in a north westward direction, it moved towards the western periphery of the high and thus into a saddle point between two anticyclonic systems (Figure 5). As Hagupit entered this position the propagation speed of the storm slowed and the tracks in the ensemble forecasts began to diverge.

5 UNCERTAINTY OF TYPHOON HAGUPIT

Stamp plots of OLR anomalies and upper level divergent wind (Figure 6) show that a convective band forms connecting Hagupit to the westerly jet. This convective band provides an outflow channel

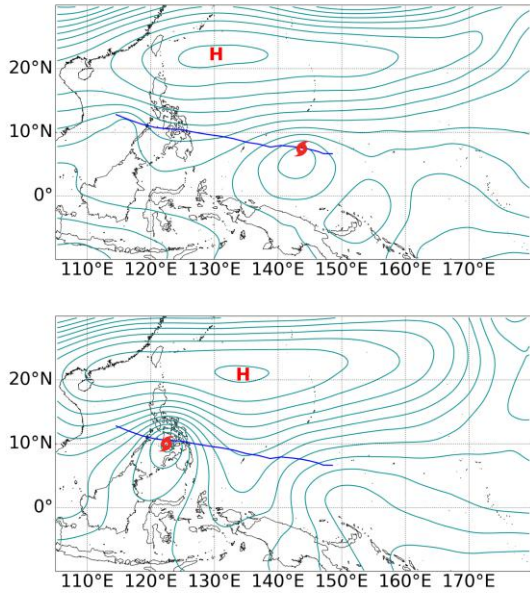


Figure 4: Global ensemble average of streamlines using a pressure-weighted average vertical level of 850 hPa-200 hPa for Haiyan at two different forecast times of (top) T+24 and (bottom) T+90.

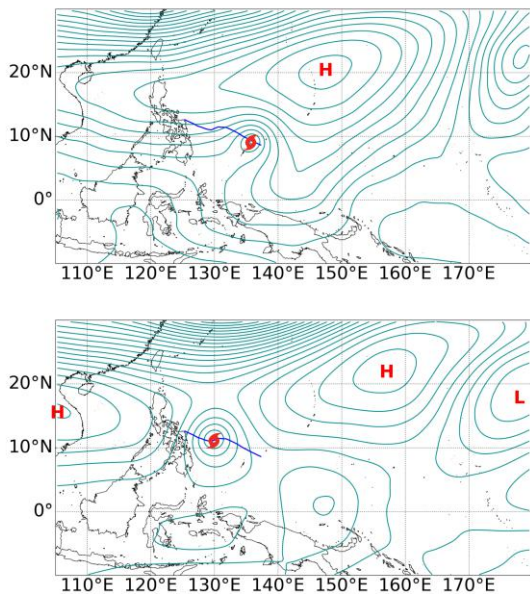


Figure 5: As in Figure 5 but for Hagupit at forecast times of (top) T+6 and (bottom) T+54.

into the mid-latitudes, as shown by the strong vertical shear and sheared 850 hPa vorticity in Figure 7. The strong vertical shear acts as a hook for the storm to turn it towards the north - as is the case in the northward turning forecasts.

From the stamp plots in Figures 6 and 7 some differences in the environment of Hagupit within the different ensemble members can be seen, how-

ever, the differences are subtle. To assess the impact of the slightly different locations of the storm in the ensemble, the TC vortex was removed following the technique described in Galarneau et al. (2013). The nondivergent and irrotational winds associated with the relative vorticity and divergence of the storm are removed from the total wind fields at a fixed radius. Following the removal of the storm the environmental winds were averaged between pressure levels. Trajectories were then calculated from the centre of the storm at T+6 and their evolution were compared to that of the track forecast. It was found that trajectories using a storm removal radius of 500-km for the global forecasts and 300-km for the 4.4-km forecasts along with a pressure-weighted average layer of 850 hPa-200 hPa were able to best predict the forecasted track of the storm (Figure 8). Figure 9 shows a vertical cross section of the azimuthal and radial velocity profiles, demonstrating the circulations which were removed in this process.

The most northerly and southerly ensemble members (10 and 5 respectively) are compared using the method described above. Figure 10 shows trajectories from these ensemble members initialised 24 hrs into the forecast, i.e. as the storm enters the region where tracks begin to diverge. The trajectories are initialised at the centre of the storm as well as two nearby locations, and are calculated after the TC vortex removal technique has been utilised. Figures 10a, 10c and 10d all show that a small change to the initial trajectory location can lead to a different track. In particular by perturbing trajectories in ensemble member 5 to the north east (i.e. towards the high pressure system), the trajectory will recurve to the north, following a path similar to the track of ensemble member 10.

6 SUMMARY

Ensemble forecasts showed large uncertainty in the track of Typhoon Hagupit after it had entered a region between two anticyclonic systems. By removing the winds associated with the TC vortex and calculating trajectories on the resulting environmental wind fields, it is shown that a small perturbation to the location of the storm upon entering this region can cause the storm to drastically change its path. Thus, due to the environment Hagupit is embedded in, a small error in location earlier in the forecast can impact on whether or not the storm recurves to the north or crosses the Philippines.

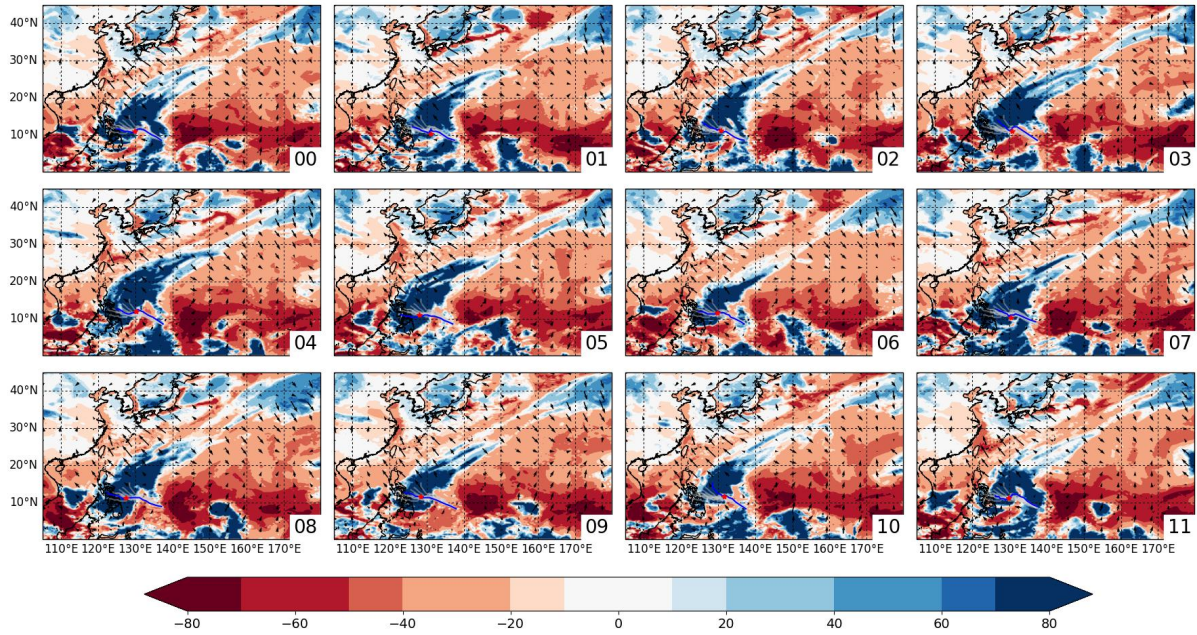


Figure 6: Ensemble stamp plot of outgoing longwave radiation (OLR) anomalies (shaded) and 200 hPa divergent wind components (arrows) for Hagupit at a valid time of 0Z, 6/12/2014. Anomalies are calculated by subtracting the OLR field from the 1974-2017 daily average using interpolated data provided by the National Oceanic and Atmospheric Administration (NOAA).

References

- Galarneau, T. J., Davis, C. A., Galarneau Jr, T. J., and Davis, C. A. (2013). Diagnosing Forecast Errors in Tropical Cyclone Motion. *Monthly Weather Review*, 141(2):405–430.
- Heming, J. T. (2017). Tropical cyclone tracking and verification techniques for Met Office numerical weather prediction models. *Meteorological Applications*, 24(1):1–8.

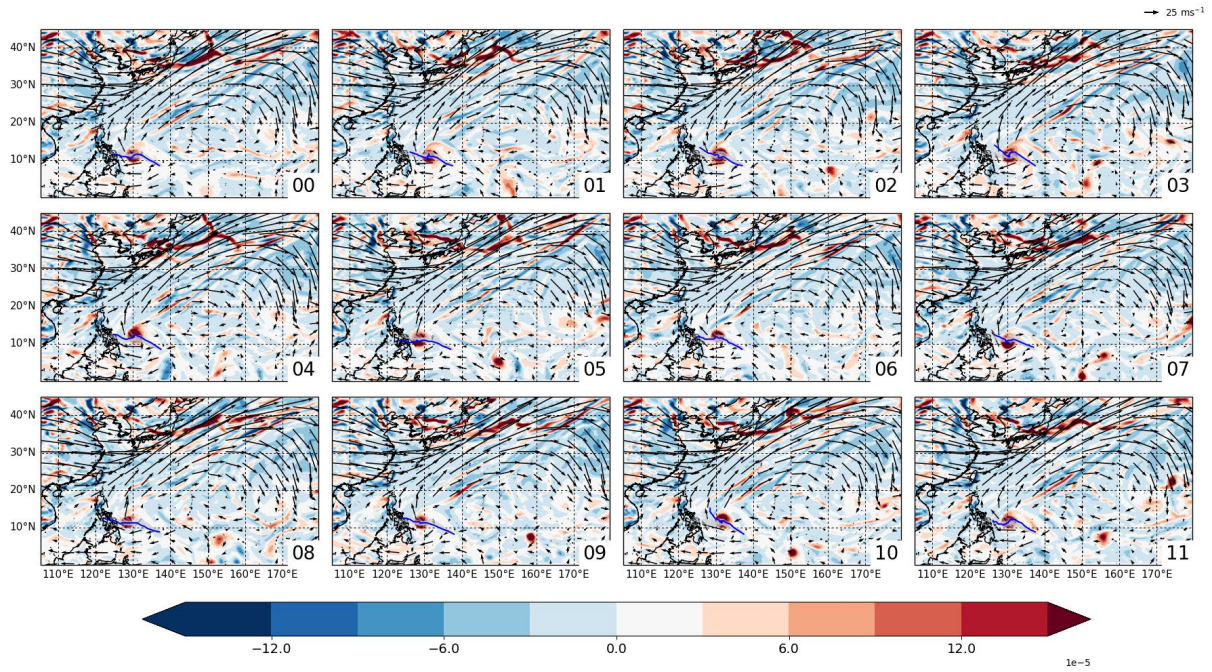


Figure 7: Ensemble stamp plot of relative vorticity at 850 hPa (shaded), vertical windshear (arrows, defined as $u_{200} - u_{850}$) and sea level pressure for Hagupit at a valid time of 0Z, 6/12/2014.

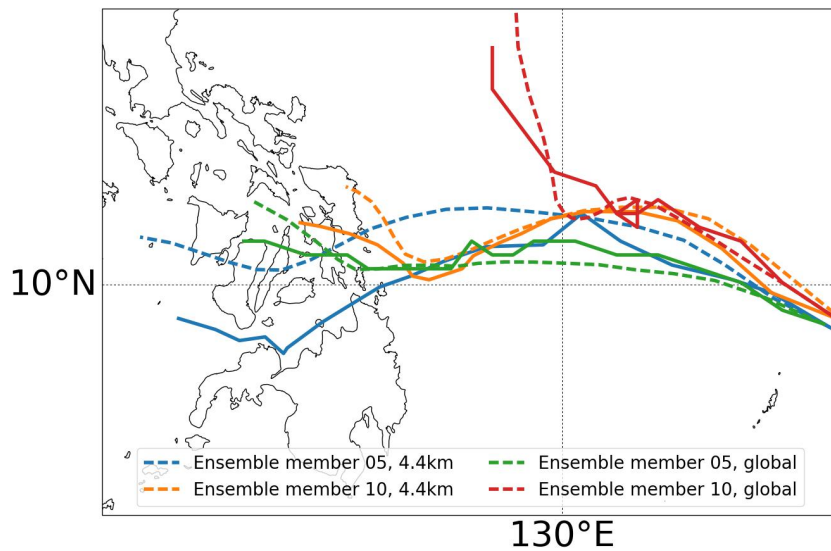


Figure 8: Comparisons of the forecast storm tracks (solid lines) and trajectories initialised from the same location after the TC vortex has been removed (dashed).

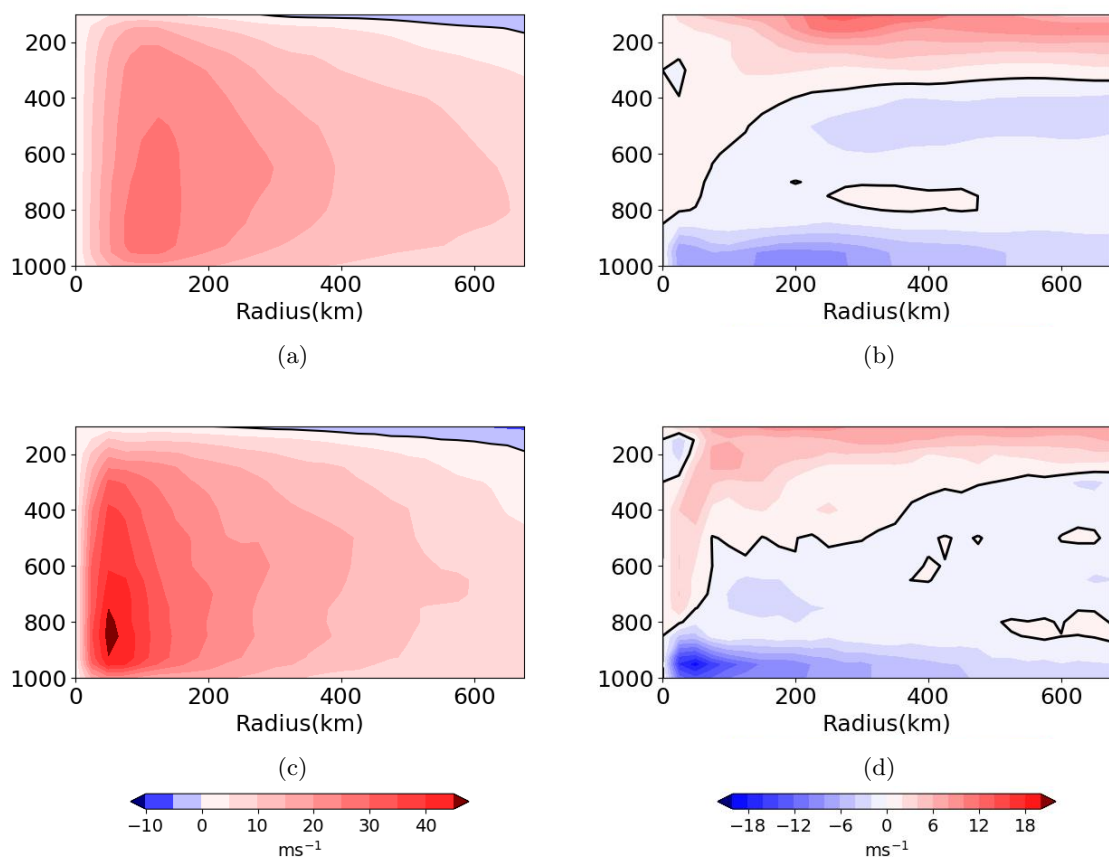


Figure 9: Azimuthal (left) and radial (right) velocities of Hagupit azimuthally averaged around the centre of the storm in the global (top) and 4.4-km (bottom) simulations at a valid time of T+48.

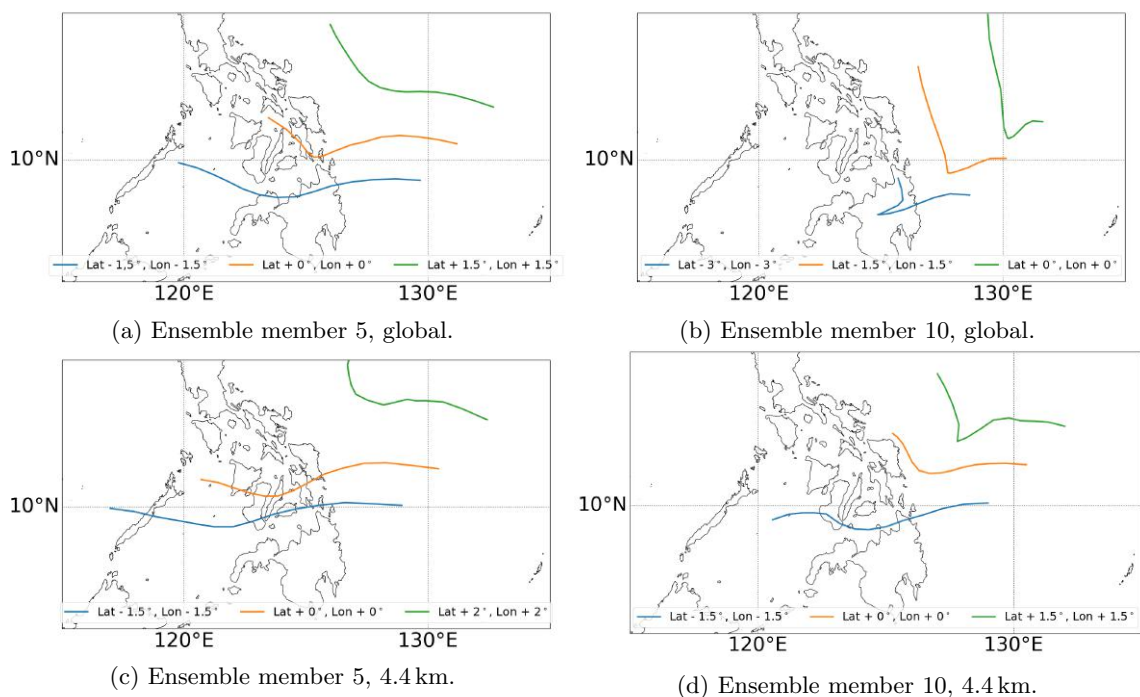


Figure 10: A trajectory comparison using the pressure-weighted average velocity between 850-200 hPa using the TC vortex removed wind fields. Trajectories are initially perturbed from the forecasted storm location by the amount shown in the legend.